[CANCER RESEARCH 64, 5527–5534, August 15, 2004]

Advances in Brief

A Mouse Skin Multistage Carcinogenesis Model Reflects the Aberrant DNA Methylation Patterns of Human Tumors

Mario F. Fraga,[1] Michel Herranz,[1] Jesús Espada,[1] Esteban Ballestar,[1] Maria F. Paz,[1] Santiago Ropero,[1] Emel Erkek,[2] Onder Bozdogan,[2] Héctor Peinado,[3] Alain Niveleau,[4] Jian-Hua Mao,[5] Alan Balmain,[5] Amparo Cano,[3] and Manel Esteller[1]

[1]Cancer Epigenetics Laboratory, Molecular Pathology Program, Spanish National Cancer Centre, Madrid, Spain; [2]Kirikkale University Faculty of Medicine, Kirikkale, Turkey; [3]Departamento de Bioquímica, Facultad de Medicina, Instituto de Investigaciones Biomédicas, Centro de Biologia Molecular "Severo Ochoa," Universidad Autonoma de Madrid, Madrid, Spain; [4]Centre Commun de Quantimetrie, Faculte de Medecine, Universite Claude Bernard Lyon I, Lyon, France; and [5]Cancer Research Institute, University of California at San Francisco, San Francisco, California

Abstract

Whereas accepted models of tumorigenesis exist for genetic lesions, the timing of epigenetic alterations in cancer is not clearly understood. We have analyzed the profile of aberrations in DNA methylation occurring in cells lines and primary tumors of one of the best-characterized mouse carcinogenesis systems, the multistage skin cancer progression model. Initial analysis using high-performance capillary electrophoresis and immunolocalization revealed a loss of genomic 5-methylcytosine associated with the degree of tumor aggressiveness. Paradoxically, this occurs in the context of a growing number of hypermethylated CpG islands of tumor suppressor genes at the most malignant stages of carcinogenesis. We have observed this last phenomenon using two approaches, a candidate gene approach, studying genes with well-known methylation-associated silencing in human tumors, and a mouse cDNA microarray expression analysis after treatment with DNA demethylating drugs. The transition from epithelial to spindle cell morphology is particularly associated with major epigenetic alterations, such as *E-cadherin* methylation, demethylation of the *Snail* promoter, and a decrease of the global DNA methylation. Analysis of data obtained from the cDNA microarray strategy led to the identification of new genes that undergo methylation-associated silencing and have growth-inhibitory effects, such as the insulin-like growth factor binding protein-3. Most importantly, all of the above genes were also hypermethylated in human cancer cell lines and primary tumors, underlining the value of the mouse skin carcinogenesis model for the study of aberrant DNA methylation events in cancer cells.

Introduction

DNA methylation is the main epigenetic modification in humans. Aberrant DNA methylation has emerged in recent years as a common hallmark of all types of cancer. Two DNA methylation lesions coexist in human neoplasms, hypermethylation of the promoter region of specific tumor suppressor genes within a context of genomic hypomethylation (1–3). It is widely accepted that a succession of accumulative hits occurring in oncogenes and tumor suppressor genes leads to genetic lesions, as represented in the elegant model of human colorectal tumorigenesis proposed by Fearon and Vogelstein (4) in 1990. However, very little is known regarding the precise timetable of epigenetic alterations occurring between the transition of a normal cell through intermediate tumorigenic stages to a tumor cell with invasive properties. To address this issue we have studied how DNA methylation changes progress in a well-established model system of mouse carcinogenesis, the multistage skin tumor progression model (reviewed in Refs. 5, 6). In this model, beginning with normal mouse skin, sequential topic application of various mutagens, such as the polycyclic aromatic hydrocarbon dimethylbenzanthracene, and tumor promoting agents, such as 12-*O*-tetra-decanoylphorbol-13-acetate, generate a spectrum of different stages of tumorigenesis ranging from premalignant papilloma to highly metastatic tumors with well-defined genetic lesions in *H-ras* or *p53* (reviewed in Refs. 5, 6). We have examined the aberrant DNA methylation profile (by candidate gene as well as genomic DNA and RNA approaches) of all stages of mouse skin tumor progression, including normal mouse skin; nontumorigenic and tumorigenic immortalized keratinocytes (MCA3D and PAM212, respectively; Refs. 7, 8); benign papilloma cells (PB and MSCP6; Refs. 9, 10); tumorigenic squamous carcinoma cells representative of different degrees of differentiation, invasion, and metastasis (PDV, MSC11B9, and HaCa4; Refs. 11–13); and highly anaplastic spindle carcinoma cell lines displaying metastatic behavior (MSC11A5, CarB, and CarC; Refs. 13, 14). Aberrantly methylated genes identified by the mouse study were confirmed in human neoplasms to evaluate the potential of this system to find clinically relevant genes with methylation-associated inactivation and also its ability to serve as a tool to improve understanding of the timing and hierarchy of epigenetic lesions in human cancer.

Materials and Methods

Mouse and Human Tumorigenic Cell Lines and Primary Tumors. The generation and culture conditions of the cell lines from the mouse skin multistage tumor progression model have been described previously (7–14). According to an increasing order of tumorigenicity activity, they included MCA3D (8, 11); PB and MSCP6 (9, 10); PDV (8, 11); PAM212 (7); MSC11B9 and MSC11A5 (13, 14); HaCa4 (12); and CarB and CarC (13, 14). Thirty human cancer cell lines corresponding to 14 cell types were obtained from the American Type Culture Collection (Rockville, MD) and the German Collection of Microorganisms and Cell Cultures (Braunschweig, Germany). Demethylating treatments were carried out using 5-aza-2-deoxycytidine (5 μM) for 48 h, with drug and medium replaced 24 h after the beginning of the treatment. Tissue samples of 86 human primary malignancies corresponding to colon, breast, lung, and head-neck carcinomas; glioma; and leukemia were also obtained at the time of clinically indicated surgical procedures, and DNA was extracted according to standard procedures. Finally, 15 primary mouse skin tumors (5 papillomas, 5 squamous carcinomas, and 5 spindle carcinomas) from the same genetic background were obtained.

Genome Content of 5-Methylcytosine. Quantification of the degree of methylation was carried out by high-performance capillary electrophoresis as described previously (15, 16). In brief, DNA samples (5 μl, 0.2–1 μg/μL) were enzymatically hydrolyzed with nuclease P1 (Sigma-Aldrich Química S.A.,

Received 12/29/03; revised 5/11/04; accepted 6/24/04.

Grant support: Health (FIS) and Science (I+D) Departments of the Spanish Government and the Asociacion Espanola contra el Cancer (AECC).

The costs of publication of this article were defrayed in part by the payment of page charges. This article must therefore be hereby marked *advertisement* in accordance with 18 U.S.C. Section 1734 solely to indicate this fact.

Note: Supplementary data for this article can be found at Cancer Research Online (http://cancerres.aacrjournals.org).

Requests for reprints: Manel Esteller, Cancer Epigenetics Laboratory, Molecular Pathology Programme, Spanish National Cancer Centre (CNIO), Melchor Fernández Almagro 3, 28029 Madrid, Spain. Phone: 34-91-2246940; Fax: 34-91-2246923; E-mail: mesteller@cnio.es.

Madrid, Spain) and alkaline phosphatase (Sigma-Aldrich Química S.A.). Samples were directly injected in a high-performance capillary electrophoresis system (P/ACE MDQ; Beckman-Coulter S.A., Madrid, Spain) connected to a data-processing station (32 Karat Software) and using an uncoated fused-silica capillary (Beckman-Coulter S.A.; 60.2 cm × 75 μm, effective length 50 cm). The running buffer was 14 mM $NaHCO_3$ (pH 9.6) containing 20 mM SDS. Running conditions were 25°C and operating voltages of 17 kV. All of the samples were analyzed in duplicate, and three analytical measurements were made per replicate. Quantification of the relative methylation of each DNA sample was determined as the percentage of mC of total cytosines: mC peak area × 100/(C peak area + mC peak area).

Immunolocalization of 5mC. Cells grown on coverslips were stained with mouse monoclonal antibodies against 5mC (kindly provided by Alain Niveleau, Universite Claude Bernard, Lyon, France) as described previously (17). Images of the nuclear immunolocalization of 5 mC were obtained in a Leica DMRA fluorescence microscope coupled to a Leica DC200 digital camera and captured with the Adobe Photoshop software. Densitometric profiles of light intensity through the orthogonal projections in the XY plane of captured images were generated by the public NIH Image software. Profiles are representative of the analysis of ~50 different nuclei in three different samples. To avoid false light signals of fluorescence stacking due to an artifactual morphology, only nuclei with a homogeneous chromatin distribution revealed after 4′,6-diamidino-2-phenylindole staining were considered in the densitometric analysis.

DNA Methylation Analysis of Particular Genes. We carried out bisulfite modification of genomic DNA as described previously (18). We established methylation status by PCR analysis of bisulfite-modified genomic DNA using two procedures. Firstly, all of the genes investigated were analyzed by bisulfite genomic sequencing of their corresponding CpG islands, as described elsewhere (19). Both strands were sequenced. The second analysis used methylation-specific PCR for all of the genes analyzed in several cancer cell lines and tissue samples, as described previously (18). We designed all of the bisulfite genomic sequencing and methylation-specific PCR primers according to genomic sequences around presumed transcription start sites of investigated genes. Primer sequences and PCR conditions for methylation analysis are included in supplementary web data.

Chromatin Immunoprecipitation. Chromatin immunoprecipitation assays were performed as described previously (19) using commercial antiacetylated histone H4 and antimethylK4 H3 antibodies (Upstate Biotechnologies). Chromatin was sheared to an average length of 0.25–1 kb for this analysis. PCR amplification was performed in 25 μl with specific primers for each of the analyzed promoters. For each promoter, the sensitivity of PCR amplification was evaluated on serial dilutions of total DNA collected after sonication (input fraction). Primer sequences are included in Supplemental Data.

Mouse cDNA Microarray. A cDNA microarray containing the National Institute on Aging/NIH Mouse 15K cDNA clone set[6] was used. Briefly, the mouse cDNA microarray consist of ~15,000 unique cDNA clones (rearrayed among 52,374 expressed sequence tags from pre- and peri-implantation embryos, E12.5 female gonad/mesonephros, and newborn ovary) and ≤50% novel genes with an average insert size of ~1.5 kb (20). Slides were scanned for Cy3 and Cy5 fluorescence using Scanarray 5000 XL (GSI Lumonics, Kanata, Ontario, Canada) and quantified using the GenePix Pro 4.0 software (Axon Instruments Inc., Union City, CA). Genes were selected to be up-regulated or down-regulated if the difference in ratio was at least 2-fold. For clustering analysis, the SOTA clustering program[7] was used, and trees were viewed using the TreeView program.

Semiquantitative Reverse Transcription-PCR Expression Analysis. We reverse-transcribed total RNA (2 μg) treated with DNase I (Ambion) using $oligo(dT)_{12-18}$ primer with Superscript II reverse transcriptase (Life Technologies, Inc.). We used 100 ng of cDNA for PCR amplification, and we amplified all of the genes with multiple cycle numbers (20–35 cycles) to determine the appropriate conditions for obtaining semiquantitative differences in their expression levels. Reverse transcription-PCR primers were designed between different exons to avoid any amplification of DNA. We also carried out PCR with *β-actin* (25 and 28 cycles) to ensure cDNA quality and loading accuracy. Primer sequences are included in Supplemental Data.

[6] Internet address: http://lgsun.grc.nia.nih.gov/.
[7] Internet address: http://bioinfo.cnio.es/cgibin/tools/clustering/sotarray.

Western Blot. Cells were harvested by centrifugation, and cell pellets were resuspended in ice-cold buffer [50 mM Tris-HCl (pH 8), 150 mM NaCl, 1% NP40, 0.5% sodium deoxycholate, and 0.1% SDS] with protease inhibitors (phenylmethylsulfonyl fluoride, leupeptin, aprotinin, and pepstatin) and incubated on ice for 5 min. One hundred μg of total cellular extract was fractionated on a 10% SDS-PAGE gel, transferred to polyvinylidene difluoride membrane (phenylmethylsulfonyl fluoride; Immobilon-P; Millipore), blocked in 10% milk in Tris buffered saline (pH 7.5) with 0.1% Tween 20 and immunoprobed with Dnmt1 (1:500), Dnmt3a (1:1000), and Dnmt3b (1:1000) antibodies (Abcam, Cambridge, United Kingdom). Horseradish peroxidase-conjugated antirabbit IgG (Amersham, Buckinghamshire, United Kingdom) at a dilution 1:3000 in [Tris buffered saline (pH 7.5) with 0.1% Tween 20] was used as the secondary antibody and β-actin (Sigma) as loading control. The signals were detected with Luminol reagent detection kit (Santa Cruz Biotechnology, Inc., Santa Cruz, CA).

Transfection Experiments and Colony Formation Assays. Transfections and colony assays were developed as described previously (19). In brief, pSV-β-galactosidase control vector and the expression vectors for the *IGFBP3* (pDNA-3 hIGFBP-3, provided by Dr. Sylvie Babajko, Hopital Saint Antoine, Paris, France) and the *CSRP2* genes (pCMV5-HA-hCRP2, provided by Dr. Axel M. Gressner, University of Aachen, Aachen, Germany), also containing neomycin resistance genes, were transfected into the T47D and HCT-116 cells, respectively, by the lipofection method. Cells were seeded in a six-well plate a day before transfection at a density of 2×10^5 cells/well. Two μg of purified plasmid DNA were transfected with LipofectAmine Plus reagent, according to the manufacturer's recommendations. The experiment was repeated three times. 24 h. After transfection, β-galactoside activity was measured in the cells carrying the control vector using a β-galactoside activity kit. Clones expressing the transfected proteins were selected in complete medium supplemented with 1 mg/ml G418, 48 h after transfection. Stable clones were maintained in complete medium with G418 (800 μg/ml). Total RNA from individual clones was extracted, and reverse transcription-PCR was performed to confirm that the clones were expressing the transfected genes. T47D and HCT-116 cells were also transfected with the vector containing no inserts and stable clones isolated. After ~16 days of selection, stable G418-resistant colonies were fixed, stained with 2% methylene blue in 60% methanol, and the average number of colonies present in each well was counted. Wild-type *p53* (pWZL-hp53 wt, Hygro) and $p16^{INK4a}$ (pLPC-hp16 wt-HA-puro) were used as additional positive controls, and mutants *p53* (pWZL-hp53-N175H, Hygro) and $p16^{INK4a}$ (pLPC-hp16 mut-HA-M53I-puro) were used as negative controls. All of the *p53* and $p16^{INK4a}$ expression vectors were provided by Dr. Manuel Serrano.

Results

5-Methylcytosine DNA Content in Cancer Cell Lines and Primary Tumors of the Mouse Skin Tumor Progression Model. It is accepted that the majority of human tumors have a diminished 5-methylcytosine DNA content when compared with normal tissue counterparts (21, 22). Here, we studied the alterations in the overall DNA methylation status in the mouse skin model of multistage carcinogenesis to determine when these changes also occur during tumor progression. We used two complementary approaches, high performance capillary electrophoresis, an analytical technique that provides an absolute measurement of 5-methylcytosine content (15, 16), and immunolocalization of 5-methylcytosine to give qualitative information on nuclear distribution (17, 23).

High-performance capillary electrophoresis analysis showed that there is a loss of 5-methylcytosine during tumor progression (Fig. 1*A*). There are two decreases visible in the 5-methylcytosine content during tumor progression: the first one occurs in the transition from nontumorigenic (MCA3D cells) to benign papilloma cells (PB and MSCP6) with a loss of 25% of the total 5-methylcytosine content. The second important hypomethylation event represented a loss of more than half (54%) of the total 5-methylcytosine genomic content: most importantly, this drop occurs when the transformed cells undergo an epithelial (MSC11B9 cells) to spindle (MSC11A5 cells) transition in

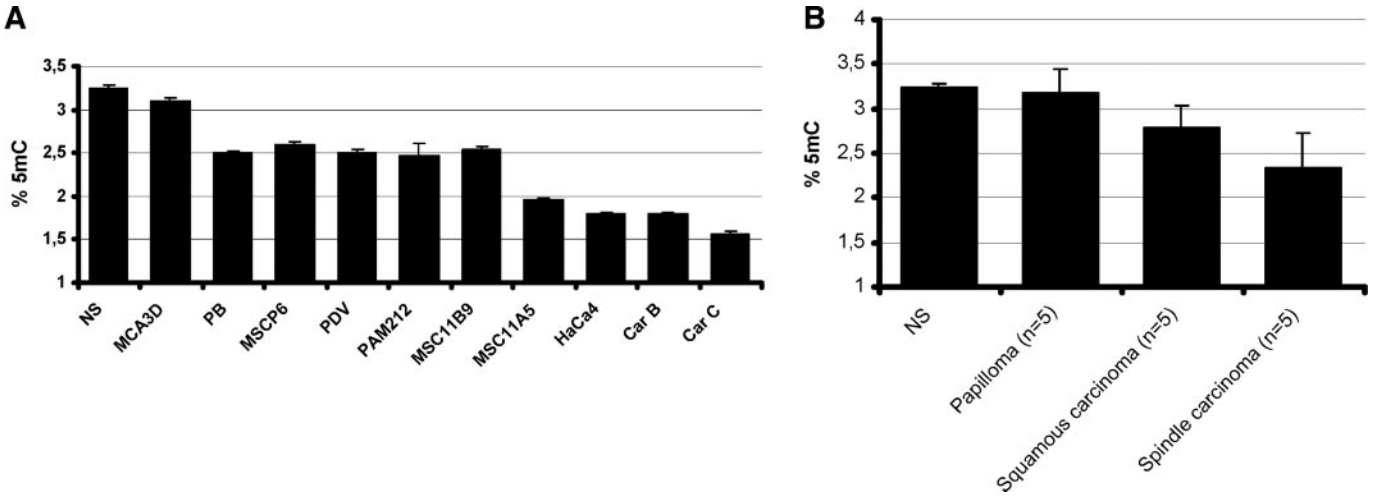

Fig. 1. Global DNA methylation status in the mouse skin tumor progression model. *A*, measurement of 5dmC content by high-performance capillary electrophoresis in mouse skin cancer cell lines as a percentage of the total cytosine pool. Results are expressed as mean; *bars*, ±SD. *B*, measurement of 5dmC content by high-performance capillary electrophoresis in mouse skin primary tumors (papillomas, $n = 5$; squamous carcinomas, $n = 5$; and spindle carcinomas, $n = 5$) as a percentage of the total cytosine pool (*right*). Results are expressed as mean; *bars*, ±SD. *NS*, normal mouse skin.

their phenotype. This morphological change is associated with a striking increase in tumorigenicity, the underlying cause of which remains unresolved.

Loss of 5-methylcytosine during the multistage carcinogenic process was also demonstrated by immunolocalization experiments. A high correlation between 5-methylcytosine levels determined by either high-performance capillary electrophoresis or immunolocalization was also observed. Interestingly, immunostaining demonstrated that the loss of 5-methylcytosine was not homogeneous within the nucleus, which is in agreement with data published previously (23).

To determine whether global DNA methylation changes observed in the cell lines of the tumor progression model could be extrapolated to primary tumors, we analyzed by high-performance capillary electrophoresis the 5-methylcytosine content of a series of primary mouse papillomas, squamous carcinomas, and spindle carcinomas (Fig. 1*B*). The data demonstrated that these skin primary tumors were hypomethylated at their DNA when compared with the normal skin. In addition, the most hypomethylated tumors were those presenting the most aggressive behavior, spindle carcinomas, in a close resemblance to our findings in the cancer cell lines. Very little decrease in methylation was detected in the primary papillomas in contrast to the results from the cell lines, but this may be due to the fact these are contaminated by stromal cells or inflammatory cells, reducing the apparent total amount of demethylation. The more cellular squamous and spindle carcinomas, however, showed a clear decrease in 5-methylcytosine content.

Analysis of Methylation-Associated Silencing of Candidate Tumor Suppressor Genes in Mouse Skin Cancer Cell Lines. To define a profile of tumor suppressor genes with methylation-associated silencing in the multistage mouse skin progression model, we analyzed the methylation status of the promoter-associated CpG island of six genes known to be hypermethylated in human cancer (1–3). These were the DNA repair genes *MLH1*, *BRCA1*, and *MGMT* (O^6-methylguanine DNA methyltransferase), the cellular adhesion-related gene *E-cadherin*, the transcriptional repressor *Snail*, and the Snail/Gfi-1 repressor family member (*MLT1*). The DNA methylation patterns were characterized by bisulfite genomic sequencing and methylation-specific PCR. Four of these genes (*MGMT*, *Snail*, *E-cadherin*, and *MLT1*) were found methylated in the mouse skin carcinogenesis model (Table 1). Methylation of the promoter regions was always associated with transcriptional silencing, and expression could be restored with the use of the demethylating agent 5-aza-2-deoxycytidine. An illustrative example of the DNA methylation and expression analysis developed is shown in Fig. 2.

Three of the four genes identified as methylated (*MGMT*, *MLT1*, and *Snail*) underwent hypermethylation at the beginning of the carcinogenic process, during the transition from fresh normal skin to immortalized nontumorigenic keratinocytes (MCA3D; Table 1). Thus, CpG island hypermethylation of candidate tumor suppressor genes is an early event in tumorigenesis.

In contrast, *E-cadherin* hypermethylation occurred in the latter stages of tumor progression coinciding with loss of epithelial phenotype (Table 1). Hypermethylation-associated silencing of *E-cadherin* is found in human tumors (1–3), but loss of *E-cadherin* expression can also result from the activity of the transcriptional repressor Snail (24). The *Snail* gene was also found to undergo epigenetic inactivation but in a different context to that of the *E-cadherin* promoter. During early stages of tumorigenesis the *E-cadherin* and *Snail* CpG islands are unmethylated and hypermethylated, respectively. However, when the transition from an epithelial (MSC11B9) to spindle (MSC11A5) or dedifferentiated (HaCa4) phenotype occurs, the *E-cadherin* promoter becomes hypermethylated, whereas the *Snail* island undergoes demethylation (Table 1). For both genes, CpG island hypermethylation

Table 1 *CpG island methylation status of candidate genes in cancer cell lines from the mouse skin tumor progression model*

	NS	MCA3D	PB	MSCP6	PDV	PAM212	MSCB119	MSC11A5	HaCa4	CarB	CarC
BRCA1	U	U	U	U	U	U	U	U	U	U	U
MLH1	U	U	U	U	U	U	U	U	U	U	U
MGMT	U	M	M	M	M	M	M	M	M	M	M
E-cadherin	U	U	U	U	U	U	U	M	M	M	M
Snail	U	M	M	M	M	M	M	U	U	U	U
MLT1	U	M	M	M	M	M	M	M	M	M	M

Abbreviations: NS, normal skin; M, methylated; U, unmethylated.

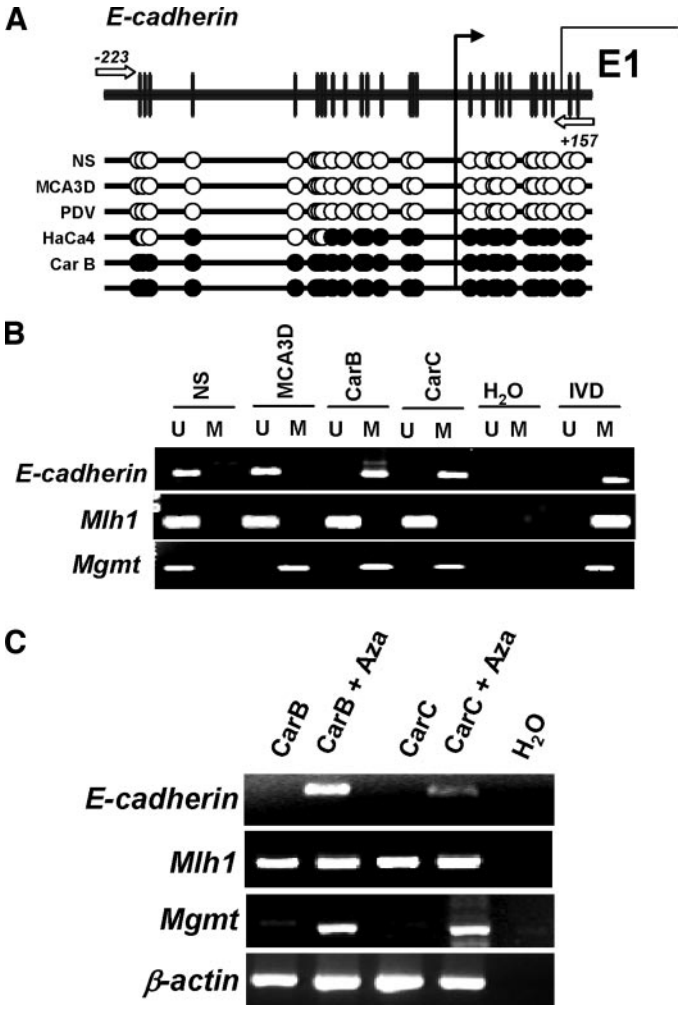

Fig. 2. CpG island methylation-associated silencing of candidate genes in the mouse tumor progression. *A*, schematic representation of the E-cadherin CpG island, where ● indicate methylated CpGs and ○ unmethylated CpGs. The *black arrows* indicate the position of the transcription start site. *B*, illustrative methylation-specific PCR analyses for the CpG island methylation status of the *E-cadherin*, *MLH1*, and *MGMT* genes. The presence of a PCR band under the *U* or *M* lane indicates unmethylated or methylated alleles, respectively. *In vitro* methylated DNA (*IVD*), used as positive methylated control and normal skin (*NS*), used as unmethylated control. *C*, examples of the reverse transcription-PCR analysis for basal gene expression and reactivation after treatment with a demethylating agent. Restoration of *E-cadherin* and *MGMT* gene expression is observed in the hypermethylated cell lines CarB and CarC after treatment with 5-aza-2-deoxycytidine. *β-Actin* expression is shown as an internal control.

was always associated with gene silencing, and expression was restored with 5-aza-2-deoxycytidine treatment as described previously.

Histone Modifications and Expression of DNA Methyltransferases in the Mouse Skin Cancer Model. Modifications in the histone tails (acetylation and methylation among others), the denominated histone code, are key in determining the active or silenced state of any given gene (25). To assess the histone modification status of the methylated and unmethylated genes analyzed in the mouse skin carcinogenesis model, we performed chromatin immunoprecipitation analysis with antibodies raised against acetylated histone H4 and dimethylated lysine 4 histone H3, both modifications associated with transcriptional activation.

We observed a loss of both acetylated histone H4 and dimethylated lysine 4 histone H3 within all of the hypermethylated CpG island promoters, whereas for both, modifications showed a significant enrichment in unmethylated CpG islands. For instance, the *MLH1* promoter, which is unmethylated and actively transcribed in all of the cell lines, was found to be associated with high amounts of both acetylated histone H4 and dimethylated lysine 4 histone H3 (Fig. 3*A*). The scenario for *E-cadherin* and *Snail*, however, was more dynamic: in the PAM212 cell line an unmethylated CpG island for *E-cadherin* was associated with enhanced amounts of acetylated histone H4 and dimethylated lysine 4 histone H3 and active transcription, whereas in CarB and CarC cells a fall of both histone modifications was associated with CpG island hypermethylation and silencing (Fig. 3*A*). For *Snail* the converse pattern was observed: methylation of the island, loss of acetylated histone H4 and dimethylated lysine 4 histone H3 and silencing in PAM212, and an unmethylated CpG island with increased acetylated histone H4 and dimethylated lysine 4 histone H3 and active transcription in CarB and CarC cells.

We then sought to determine the pattern of expression of the DNA methyltransferases (Fig. 3*B*) throughout the progression model. The expression of DNA methyltransferase 1 and DNA methyltransferase 3b was studied by Western blot using nuclear extracts obtained from cells across the spectrum of different mouse skin carcinogenesis stages. We found elevated levels of both DNA methyltransferases from early to late stages of tumorigenesis. For example, the highly metastatic cell line CarC had a 4-fold increase in DNA methyltransferase 1 and DNA methyltransferase 3b compared with just the immortalized MDA3D cells, whereas intermediate stages (such as PAM212 cell line) also had intermediate levels of DNA methyltransferase 1/3b protein (2-fold increase *versus* MDA3D; Fig. 3*B*).

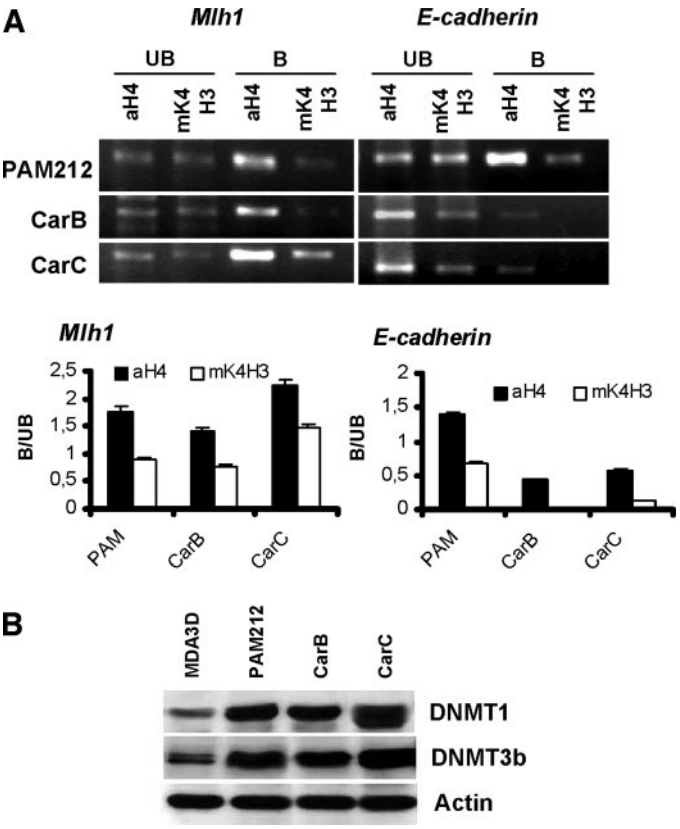

Fig. 3. Pattern of histone modifications and expression of DNA methyltransferases (*DNMT*) in the mouse skin tumorigenesis model. *A*, chromatin immunoprecipitation analysis of the histone modification status of the *MLH1* and *E-cadherin* promoters. The unbound (*UB*) and bound (*B*) fractions of each chromatin immunoprecipitation experiment are shown. Each graph shows the B:UB ratio for each studied promoter. In the cell line PAM212 an unmethylated promoter of E-cadherin is enriched in acetylated histone H4 and methyl-K4-H3, both markers of active transcription, whereas in the E-cadherin methylated cell lines CarB and CarC both markers are depleted. *B*, Western blot analysis for DNMT1 and DNMT3b expression in MCA3D, PAM212, CarB, and CarC cell lines; *bars*, ±SD.

Thus, CpG island hypermethylation of tumor suppressor genes is not an isolated phenomenon in the epigenetics of cancer progression, because it occurs in a context of disturbance in the histone and DNA methylation machinery.

Identification of Methyl-Targeted Genes by DNA Demethylating Treatment and Mouse cDNA Microarray Analysis. To obtain a global view of the number of genes epigenetically silenced throughout the different stages of mouse skin tumorigenesis, we hybridized differentially labeled RNA from each untreated cell line *versus* the same cell line after treatment with 5-aza-2-deoxycytidine to a mouse cDNA microarray containing 15,000 clones. The efficiency of the demethylating treatment was measured by the determination of the 5-methylcytosine content by high-performance capillary electrophoresis (15, 16) and by the reactivation of the methylation-associated genes as described above. This is described in the flowchart in Fig. 4*A*.

cDNA microarray expression analysis showed that after treatment with 5-aza-2-deoxycytidine, the cell lines representing early stages of carcinogenesis such as MCA3D or PAM212 show a reactivation of 2.1% and 2.4% of genes, respectively, whereas those representative of advanced stages, such as CarB and CarC, had a restoration of expression of 4.6% and 5.8% genes, respectively (Fig. 4*B*). Clustering analysis of the pattern of expression after demethylation treatment also yielded a profile that allowed discrimination between early (MCA3D and PAM212) and advanced (CarB and CarC) tumorigenesis (Fig. 4*C*).

Analysis of the expression microarray data revealed 86 candidate sequences with a more than 3-fold increase after treatment with 5-aza-2-deoxycytidine (Fig. 4*A*). From these clones, 18 genes with putative tumor suppressor-like activities were selected, 10 of which contained a CpG island within their promoter region. We analyzed the possible methylation-associated silencing of four genes from this group: the gene encoding the LIM domain protein CRP2 molecular adapter (*CSRP2*; Ref. 26), the insulin-like growth factor binding protein-3 (*IGFBP3*; Ref. 27), the chemokine receptor *CMKAR4* (28), and the antioxidant enzyme peroxiredoxin-1 (*PRDX1*; Ref. 29). CpG island hypermethylation was found to be present in the promoters of *IGFBP3*, *CMKAR4*, and *PRDX1* genes at different stages of the mouse skin carcinogenesis model, in both cancer cell lines and primary tumors (Table 2; Supplemental Data). Hypermethylation of *CSRP2* was only found in 1 of 10 mouse skin tumor cell lines. The presence of promoter hypermethylation was associated with transcriptional repression in all of the cases, which was relieved by the use of 5-aza-2-deoxycytidine. The representative detailed methylation and expression analysis for the *IGFBP3* gene is shown as an example in Fig. 4*D*.

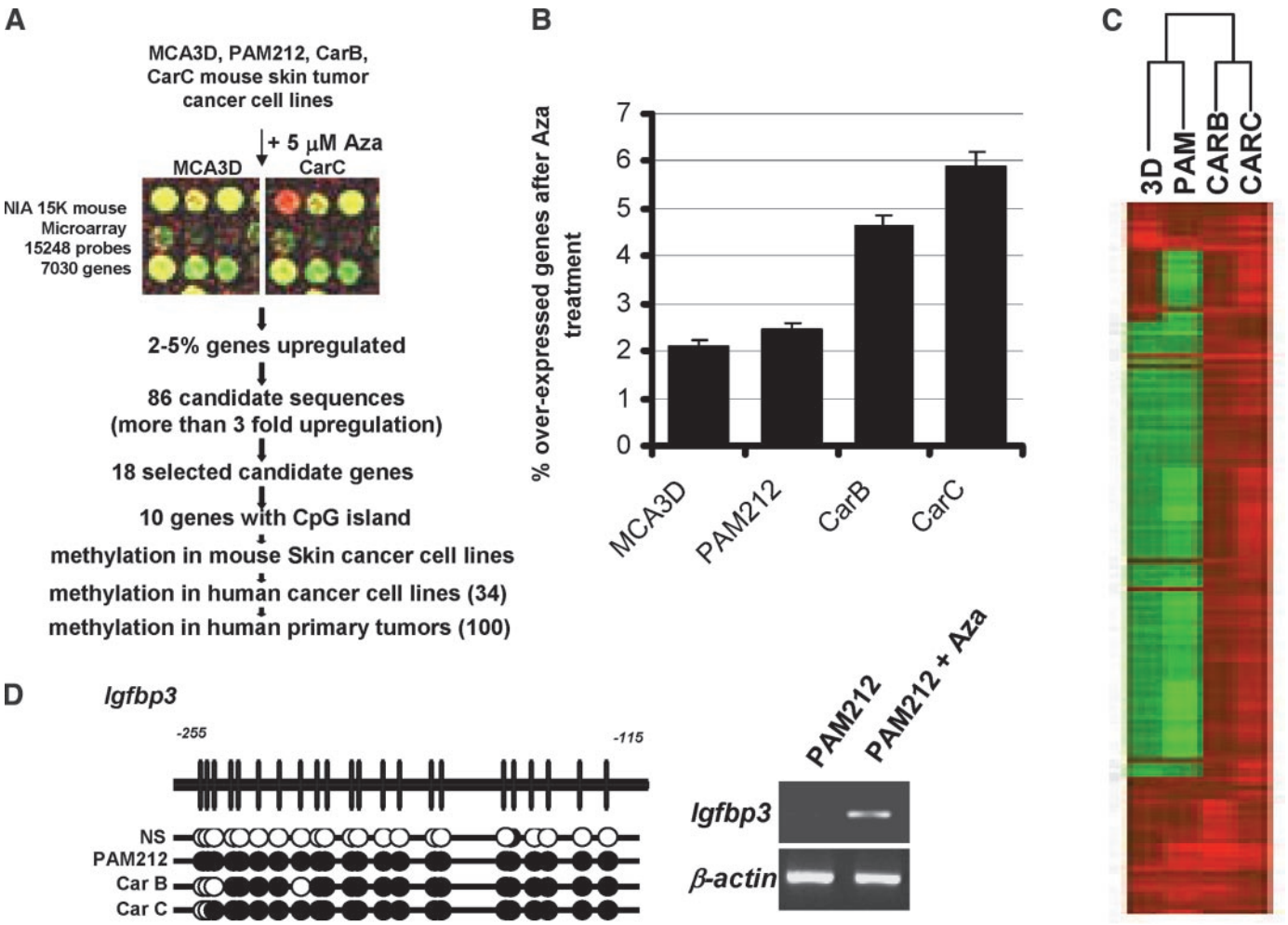

Fig. 4. Searching for new hypermethylated genes by combining cDNA microarray technology with 5-aza-2-deoxycytidine treatment. *A*, flowchart for the identification of new genes with methylation-associated silencing. *B*, percentage of overexpressed genes after treatment with 5-aza-2-deoxycytidine in the tumor progression model. *C*, aggregative hierarchical clustering of the expression data obtained. *D*, example of the detailed analysis of one of the genes identified using the above described approach, *IGFBP3*. *Up*, bisulfite genomic sequencing analysis of the *IGFBP3* CpG island; *down*, reactivation of *IGFBP3* expression by treatment with the demethylating drug. *β-Actin* expression is shown as an internal control; *bars*, ±SD.

The Aberrant DNA Methylation Pattern Observed in Mouse is Mimicked by Human Nonmelanoma Skin Cancer. We used first an equivalent cell line progression model in humans to the mouse skin multistage, consisting in three different stages of nonmelanoma human skin cancer: normal skin, immortal nontumorigenic human keratinocytes (HaCaT; Ref. 30), and high-grade malignant human epidermoid carcinoma cells (A431; Ref. 31). Similarly to the mouse, we found an increased loss of 5-methylcytosine DNA genomic content associated with the increased tumorigenic activity: HaCaT showed a 15% reduction of 5-methylcytosine DNA content *versus* the normal skin, whereas the aggressive cell line A431 displayed a 25% drop.

Related to CpG island methylation, we studied the methylation status of the four new identified methylation-positive genes in the mouse model (*CSRP2*, *IGFBP3*, *CMKAR4*, and *PRDX1*) in these three human skin samples. The last three genes were found hypermethylated in the nonmelanoma skin cancer cell line A431, whereas all four were unmethylated in normal skin and nontumorigenic keratinocytes. *CSRP2* was found unmethylated in A431. Most important, the presence of aberrant CpG island methylation was not a cell culture phenomena, because we found CpG island promoter hypermethylation of these genes in a significant proportion, from 58% to 12%, of primary nonmelanoma human skin tumors ($n = 26$; Table 2).

Methylation-Associated Silencing Outside Skin Tumors. To obtain a comprehensive view of the relevance of the methylation status of *CSRP2*, *IGFBP3*, *CMKAR4*, and *PRDX1* outside skin tumors, we screened a large panel of cancer cell lines ($n = 28$) and primary tumors ($n = 83$) from a wide variety of cell types.

All four of the identified methylation-positive genes in the mouse model were methylated in a significant proportion of human cancer cell lines (Table 2; Supplemental Data). In all of the cases, the presence of methylation was associated with gene silencing, and reactivation by 5-aza-2-deoxycytidine was demonstrated. The illustrative case for *CSRP2* with bisulfite genomic sequencing, methylation-specific PCR analysis and expression study is shown in Fig. 5. CpG island promoter hypermethylation of *IGFBP3* was the most common event, being present in 60% (17 of 28) of cancer cell lines from different cell types (Table 2).

We tested the relevance of these aberrant methylation lesions not only in *in vitro* cultured cancer cells but also *in vivo* in samples taken from cancer patients. For this purpose we analyzed the CpG island methylation status of the four selected candidate genes (*CSRP2*, *IGFBP3*, *CMKAR4*, and *PRDX1*) in human primary tumors ($n = 83$), including all of the major common cell types (breast, colon, lung, brain, head and neck cancer, and leukemia; Table 2; Supplemental Data). *CSRP2*, *IGFBP3*, *CMKAR4*, and *PRDX1* were found significantly hypermethylated across the spectrum of primary tumors. From a quantitative standpoint, *IGFBP3* CpG island hypermethylation was the most common epigenetic alteration, similar to the cell lines, being found in 57% (37 of 65) of all of the primary malignancies (Table 2). Most interesting, a tumor type-specific profile was observed, for example the chemokine inhibitor *CMKAR4* was methylated in leukemia but not in mammary or colon tumors (Supplemental Data).

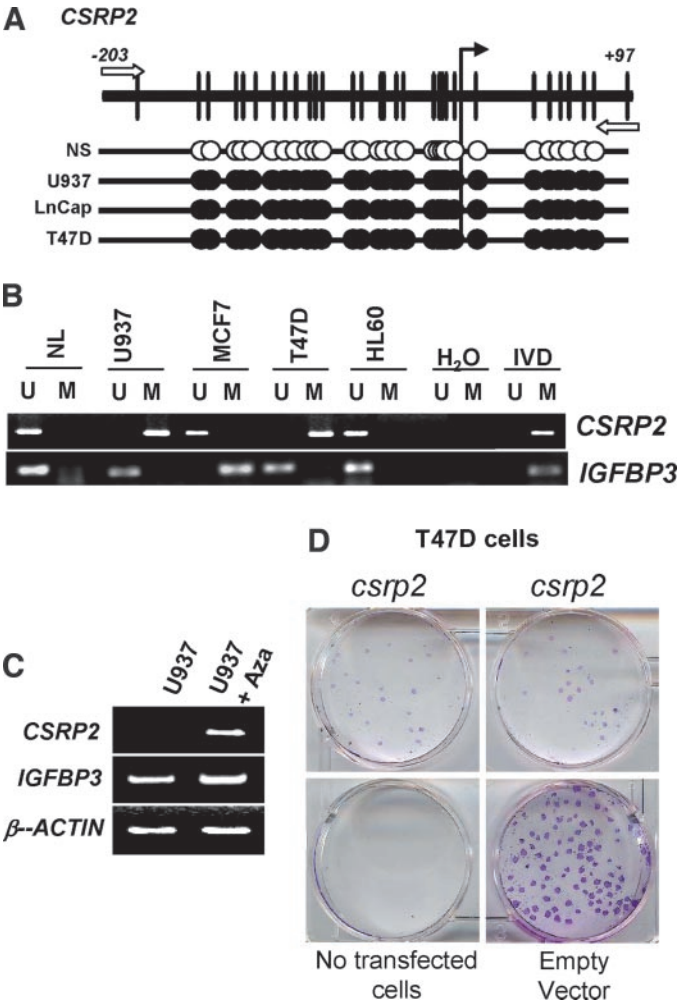

Fig. 5. Examples of methylation-associated silencing of the corresponding human genes derived from the mouse cDNA microarray approach. *A*, bisulfite genomic sequencing of the *CSRP2* CpG island in human normal skin (*NS*), normal lymphocytes (*NL*), and different cancer cell lines. *B*, methylation specific-PCR analysis of the *CSRP2* and *IGFBP3* CpG islands in human normal skin (*NS*), normal lymphocytes (*NL*), and different cancer cell lines. *C*, reactivation of *CSRP2* expression in a hypermethylated cell line by treatment with the demethylating drug. *D*, colony formation assay for *CSRP2*. *CSRP2* methylation-silenced cells (T47D) were transfected with a *CSRP2* expression vector or the empty vector as explained in "Materials and Methods."

Growth-Inhibitory Effects in Human Cancer Cells. Finally, to gain additional insight into the potential role and relevance of these hypermethylated genes for tumor formation, we reintroduced *CSRP2* and *IGFBP3* in the human breast and colorectal cancer cell lines T47D and HCT-116, respectively, in which we had demonstrated inactivation by hypermethylation. Overexpressing a previously silenced gene product to measure the tumor suppressing-like activity has been successfully applied recently to other methylation-silenced genes, such as *SEMA3B*, *SOCS-1*, or *CRIP1* (32–34). After selection

Table 2 *Percentage of CpG island hypermethylation in mouse and human cancer samples for the identified new target genes*

	Mouse				Human		
		Mouse skin primary tumors ($n = 15$)				Human primary tumors ($n = 109$)	
	Mouse skin tumor cell lines ($n = 10$)	Papilloma ($n = 5$)	Squamous carcinoma ($n = 5$)	Spindle carcinoma ($n = 5$)	Human cancer cell lines ($n = 28$)	Nonmelanoma skin tumors ($n = 26$)	Other tumors ($n = 83$)
IGFBP3	3/10 (30%)	0/5	2/5 (40%)	4/5 (80%)	17/28 (60.27%)	3/25 (12%)	37/65 (57%)
CMKAR4	8/10 (80%)	0/5	1/5 (20%)	1/5 (20%)	10/28 (36%)	8/26 (31%)	9/70 (13%)
PRDX1	3/10 (30%)	0/5	0/5	1/5 (20%)	4/28 (14%)	14/24 (58%)	2/74 (3%)
CSRP2	1/10 (10%)	0/5	0/4	0/5	4/28 (14%)	6/24 (25%)	11/70 (16%)

of drug-resistant colonies and the demonstration that each gene was re-expressed, we found that the genetic restoration of any of these genes was sufficient to significantly decrease colony formation, 80% for *CSRP2* and 90% for *IGFBP3*, as did our positive control *p53* (95% reduction) or $p16^{INK4a}$ (90% reduction), but not in the case of the mutant *p53* or $p16^{INK4a}$ forms or the empty vectors. A representative experiment for *CSRP2* is shown in Fig. 5*D*.

Discussion

In the genesis and progression of cancer an interplay between genetic and environmental factors occurs. Epigenetics, understood as a mechanism of conferring heritable states of gene expression without altering the DNA sequence, is now established as an important factor in tumorigenesis, largely represented by DNA methylation and histone modifications. Although CpG island hypermethylation-associated silencing of tumor suppressor genes (*BRCA1*, *MLH1*, and so forth) and global genomic hypomethylation are accepted as playing a fundamental role in cancer we are still in the early stages of understanding the timing and hierarchy of epigenetic lesions and their cross-talk with genetic and environmental factors. We have defined the DNA methylation status of a well-known carcinogenic system, the mouse skin multistage progression model (7–14), and demonstrated the cumulative appearance of aberrant DNA methylation and its lesions.

It is clear that the genome-wide loss of 5-methylcytosine is a molecular hallmark associated with the acquisition of a transformed phenotype. The first decrease in overall 5-methylcytosine levels was seen during the early stages of benign tumor growth. A second, more precipitous drop occurred when the cancer cells changed from an epithelial phenotype to a highly metastatic dedifferentiated/spindle morphology. These data support the use of genomic hypomethylation levels as a biomarker of tumor aggressiveness. These results confirm that global genomic hypomethylation does not exist as a static predefined value throughout the process of carcinogenesis but rather as a dynamic parameter. Our data, together with recent experiments showing an enhanced tumorigenicity and chromosomal instability in the mouse with hypomorphic alleles of the DNA methyltransferases (35), suggests an important role for DNA hypomethylation in malignant transformation.

Cancer epigenetics studies cannot be fully understood if we do not determine the relevance of the silencing of tumor suppressor genes associated with CpG island hypermethylation and its histone modifications and chromatin-linked changes. In this study, using candidate gene and demethylating microarray expression approaches, we have shown that cancer cells accumulate methylation-mediated gene silencing from the early to the advanced carcinogenic stages. Whereas normal skin (or any other normal tissue) presents unmethylated CpG islands, in the earliest step in the process, when we just established immortalized cells (MCA3D), numerous gene promoters become hypermethylated and silenced. Thus, it has also been suggested by the finding of gene hypermethylation in static studies of premalignant lesions, such as colorectal and gastric adenomas, uterine hyperplasias, or ulcerative colitis (2), the epigenetic silencing of tumor suppressor genes is one of the most precocious hits in tumorigenesis.

A dynamic profile of CpG island methylation within a set of a set of genes involved in cell adhesion can be especially relevant to the process of metastasis. E-cadherin is a protein largely involved in cell-cell adhesion of epithelial tissues. Loss of *E-cadherin* expression has been casually linked to acquisition of invasiveness, and *E-cadherin* methylation-associated silencing occurs in human cancer (2, 3). Interestingly, the subsequent growth of metastases in secondary organs has been related to its re-expression in these distal sites (36), and reactivation by demethylation occurs in cancer cells grown in spheroids, which requires homotypic cell adhesion (37). In the mouse skin carcinogenesis model, the methylation of *E-cadherin* was the single event that most clearly marked the change from epithelial to dedifferentiated HaCa4 cells, and is therefore in close agreement with the previously described pattern of *E-cadherin* expression in this model associated with the acquisition of a metastatic phenotype (38). Lending additional support to the idea of epigenetic plasticity, *E-cadherin* hypermethylation at the latter stages of tumorigenesis was associated with the demethylation of its transcriptional repressor *Snail*, so that it had methylation-associated silencing at the early stages. The dynamics of *Snail* CpG island methylation is also in strict agreement with its expression pattern during mouse skin tumor progression (24). Furthermore, Snail recruits histone deacetylase activity to the *E-cadherin* promoter (39), which, in turn, associates with DNA methyltransferases. Therefore, the epigenetic reactivation of Snail in late stages of tumorigenesis may promote the hypermethylation of the *E-cadherin* CpG island and lead to full silencing in an example of cross-talk between epigenetic events.

At this point it is important to stress the relevance of the multistage mouse skin carcinogenesis model (reviewed in Refs. 5, 6) as a tool for a better understanding human cancer epigenetics and assisting the development of new anticancer agents. First, genes with known methylation-associated silencing in human tumors (*MGMT*, *E-cadherin*, and so forth) were also found epigenetically inactive in the mouse tumors. Secondly, microarray analysis of mouse cancer cells treated with demethylating agents revealed new set of genes with not only methylation-associated silencing in mouse tumors but also in human primary cancer. These target genes include, among others, the insulin-like growth factor binding protein 3 (*IGFBP3*), a mediator of apoptosis with antiproliferative signaling effect (27); the chemokine receptor *CMKAR4*, implicated in tumor adhesion to microvascular endothelial cells (28); the 1-Cys peroxiredoxin (*PRDX1*), involved in the defense against oxidant stress (29); or the cell differentiating factor cysteine-rich protein 2 (*CSRP2*; Ref. 26). An evaluation of the tumor suppressor-like activities of these genes has just begun, and mutation screening of these genes in cancer cells is reported in the literature, but each one will merit a more profound study to establish their contribution to tumorigenesis and their potential as biomarkers of the disease.

Finally, similar epigenetic behavior observed in multistage skin tumor progression compared with human cancer cell lines and both mouse and human primary tumors may herald the mouse model as an excellent system to test all current and newly produced anticancer drugs targeting epigenetics (reviewed in Ref. 3). We are in the early stages of the development of DNA demethylating drugs and inhibitors of histone deacetylases for the treatment of cancer, although clinical studies using these agents have been initiated worldwide. The versatility of the mouse carcinogenesis model now offers a safe and convenient environment to test these compounds for clinical efficacy and toxic side effects.

References

1. Jones PA, Laird PW. Cancer epigenetics comes of age. Nat Genet 1999;21:163–7.
2. Esteller M. CpG island hypermethylation and tumor suppressor genes: a booming present, a brighter future. Oncogene 2002;21:5427–40.
3. Herman JG, Baylin SB. Gene silencing in cancer in association with promoter hypermethylation. N Engl J Med 2003;349:2042–54.
4. Fearon ER, Vogelstein B. A genetic model for colorectal tumorigenesis. Cell 1990; 61:759–67.
5. Yuspa SH. The pathogenesis of squamous cell cancer: lessons learned from studies of skin carcinogenesis–thirty-third G. H. A. Clowes Memorial Award Lecture. Cancer Res 1994;54:1178–89.
6. Balmain A, Harris CC. Carcinogenesis in mouse and human cells: parallels and paradoxes. Carcinogenesis 2000;21:371–7.
7. Yuspa SH, Hawley-Nelson P, Koehler B, Stanley JR. A survey of transformation markers in differentiating epidermal cell lines. Cancer Res 1980;40:4694–703.

8. Kulesz-Martin M, Klikenney AE, Holbrook KA, Digernes V, Yuspa SH. Properties of carcinogen altered mouse epidermal cells resistant to calcium induced terminal differentiation. Carcinogenesis 1983;4:1367–77.
9. Yuspa SH, Morgan D, Lichti U, et al. Cultivation and characterization of cells derived from mouse skin papillomas induced by initiation-promotion protocol. Carcinogenesis 1986;7:949–58.
10. Haddow S, Fowlis SD, Parkinson K, Akhurst RJ, Balmain A. Loss of growth control by TGF-beta occurs at a late stage of mouse skin carcinogenesis and is independent of ras gene activation. Oncogene 1991;6:1465–70.
11. Fusenig N, Breitkreutz D, Dzarlieva R, et al. Epidermal cell differentiation and malignant transformation in culture. Cancer Forum 1982;6:209–40.
12. Brown K, Quintanilla M, Ramsden M, Kerr IB, Young S, Balmain A. v-ras genes from harvey and BALB murine sarcoma viruses can act as initiators of two-stage mouse skin carcinogenesis. Cell 1986;46:447–56.
13. Burns PA, Kemp CJ, Gannon JV, Lane DP, Bremner R, Balmain A. Loss of heterozigosity and mutational alterations of the p53 gene in skin tumors of interspecific hybrid mice. Oncogene 1991;6:2363–9.
14. Buchmann A, Ruggeri B, Klein-Szanto AJP, Balmain A. Progression of squamous carcinoma cells to spindle carcinomas of mouse slin is associated with an imbalance of H-ras alleles on chromosome 7. Cancer Res 1991;51:4097–101.
15. Fraga MF, Uriol E, Diego LB, et al. High-performance capillary electrophoretic method for the quantification of 5-methyl 2′-deoxycytidine in genomic DNA: application to plant, animal and human cancer tissues. Electrophoresis 2002;23:1677–81.
16. Paz MF, Fraga MF, Avila S, et al. A systematic profile of DNA methylation in human cancer cell lines. Cancer Res 2003;63:1114–21.
17. Habib M, Fares F, Bourgeois CA, et al. DNA global hypomethylation in EBV-transformed interphase nuclei. Exp Cell Res 1999;249:46–53.
18. Herman JG, Graff JR, Myohanen S, Nelkin BD, Baylin SB. Methylation-specific PCR: a novel PCR assay for methylation status of CpG islands. Proc Natl Acad Sci USA 1996;93:9821–6.
19. Ballestar E, Paz MF, Valle L, et al. Methyl-CpG binding proteins identify novel sites of epigenetic inactivation in human cancer. EMBO J 2003;22:6335–45.
20. Tanaka TS, Jaradat SA, Lim MK, et al. Genome-wide expression profiling of mid-gestation placenta and embryo using 15k mouse developmental cDNA microarray. Proc Natl Acad Sci USA 2000;97:9127–32.
21. Feinberg AP, Vogelstein B. Hypomethylation distinguishes genes of some human cancers from their normal counterparts. Nature 1983;301:89–92.
22. Ehrlich M. DNA hypomethylation in cancer. In: Ehrlich M, editor. DNA alterations in cancer: genetic and epigenetic changes. Natick: Eaton Publishing; 2000. p. 273–91.
23. Hernandez-Blazquez FJ, Habib M, Dumollard JM, et al. Evaluation of global DNA hypomethylation in human colon cancer tissues by immunohistochemistry and image analysis. Gut 2000;47:689–93.
24. Cano A, Perez-Moreno MA, Rodrigo I, et al. The transcription factor snail controls epithelial-mesenchymal transitions by repressing E-cadherin expression. Nat Cell Biol 2000;2:76–83.
25. Ballestar E, Esteller M. The impact of chromatin in human cancer: linking DNA methylation to gene silencing. Carcinogenesis 2002;23:1103–9.
26. Weiskirchen R, Gunther K. The CRP/MLP/TLP family of LIM domain proteins: acting by connecting. Bioessays 2003;25:152–62.
27. Baxter RC. Signalling pathways involved in antiproliferative effects of IGFBP-3: a review. Mol Pathol 2001;54:145–8.
28. Murakami T, Maki W, Cardones AR, et al. Expression of CXC chemokine receptor-4 enhances the pulmonary metastatic potential of murine B16 melanoma cells. Cancer Res 2002;62:7328–34.
29. Manevich Y, Sweitzer T, Pak JH, Feinstein SI, Muzykantov V, Fisher AB. 1-Cys peroxiredoxin overexpression protects cells against phospholipid peroxidation-mediated membrane damage. Proc Natl Acad Sci USA 2002;99:11599–604.
30. Boukamp P, Petrussevska RT, Breitkreutz D, Hornung J, Markham A, Fusenig NE. Normal keratinization in a spontaneously immortalized aneuploid human keratinocyte cell line. J Cell Biol 1988;106:761–71.
31. Giard DJ, Aaronson SA, Todaro GJ, et al. In vitro cultivation of human tumors: establishment of cell lines derived from a series of solid tumors. J Natl Cancer Inst 1973;51:1417–23.
32. Tomizawa Y, Sekido Y, Kondo M, et al. Inhibition of lung cancer cell growth and induction of apoptosis after reexpression of 3p21.3 candidate tumor suppressor gene SEMA3B. Proc Natl Acad Sci USA 2001;98:13954–9.
33. Yoshikawa H, Matsubara K, Qian GS, et al. SOCS-1, a negative regulator of the JAK/STAT pathway, is silenced by methylation in human hepatocellular carcinoma and shows growth-suppression activity. Nat Genet 2001;28:29–35.
34. Yamashita K, Upadhyay S, Osada M, et al. Pharmacologic unmasking of epigenetically silenced tumor suppressor genes in esophageal squamous cell carcinoma. Cancer Cell 2002;2:485–95.
35. Gaudet F, Hodgson JG, Eden A, et al. Induction of tumors in mice by genomic hypomethylation. Science 2003;300:489–92.
36. Takeichi M. Cadherin cell adhesion receptors as a morphogenetic regulator. Science 1991;251:1451–5.
37. Graff JR, Gabrielson E, Fujii H, Baylin SB, Herman JG. Methylation patterns of the E-cadherin 5′ CpG island are unstable and reflect the dynamic, heterogeneous loss of E-cadherin expression during metastatic progression. J Biol Chem 2000;275:2727–32.
38. Navarro P, Gomez M, Pizarro A, Gamallo C, Quintanilla M, Cano A. A role for the E-cadherin cell-cell adhesion molecule during tumor progression of mouse epidermal carcinogenesis. J Cell Biol 1991;115:517–33.
39. Peinado H, Ballestar E, Esteller M, Cano A. The transcription factor Snail mediates E-cadherin repression by the recruitment of the Sin3A/Histone Deacetylase 1/2 complex. Mol Cell Biol 2004;24:306–19.

A Mouse Skin Multistage Carcinogenesis Model Reflects the Aberrant DNA Methylation Patterns of Human Tumors

Mario F. Fraga, Michel Herranz, Jesús Espada, et al.

Cancer Res 2004;64:5527-5534.